Published in final edited form as:
*J Comp Neurol*. 2008 November 10; 511(2): 221–237. doi:10.1002/cne.21829.

# The Medial Paralemniscal Nucleus and Its Afferent Neuronal Connections in Rat

**TAMÁS VARGA**[1], **MIKLÓS PALKOVITS**[1], **TED BJÖRN USDIN**[2], and **ARPÁD DOBOLYI**[1,*]

[1]Neuromorphological and Neuroendocrine Research Laboratory, Department of Anatomy, Histology and Embryology, Semmelweis University and the Hungarian Academy of Sciences, Budapest, H-1094, Hungary

[2]Section on Fundamental Neuroscience, National Institute of Mental Health, Bethesda, Maryland 20892

## Abstract

Previously, we described a cell group expressing tuberoinfundibular peptide of 39 residues (TIP39) in the lateral pontomesencephalic tegmentum, and referred to it as the medial paralemniscal nucleus (MPL). To identify this nucleus further in rat, we have now characterized the MPL cytoarchitectonically on coronal, sagittal, and horizontal serial sections. Neurons in the MPL have a columnar arrangement distinct from adjacent areas. The MPL is bordered by the intermediate nucleus of the lateral lemniscus nucleus laterally, the oral pontine reticular formation medially, and the rubrospinal tract ventrally, whereas the A7 noradrenergic cell group is located immediately mediocaudal to the MPL. TIP39-immunoreactive neurons are distributed throughout the cytoarchitectonically defined MPL and constitute 75% of its neurons as assessed by double labeling of TIP39 with a fluorescent Nissl dye or NeuN. Furthermore, we investigated the neuronal inputs to the MPL by using the retrograde tracer cholera toxin B subunit. The MPL has afferent neuronal connections distinct from adjacent brain regions including major inputs from the auditory cortex, medial part of the medial geniculate body, superior colliculus, external and dorsal cortices of the inferior colliculus, periolivary area, lateral preoptic area, hypothalamic ventromedial nucleus, lateral and dorsal hypothalamic areas, subparafascicular and posterior intralaminar thalamic nuclei, periaqueductal gray, and cuneiform nucleus. In addition, injection of the anterograde tracer biotinylated dextran amine into the auditory cortex and the hypothalamic ventromedial nucleus confirmed projections from these areas to the distinct MPL. The afferent neuronal connections of the MPL suggest its involvement in auditory and reproductive functions.

### Keywords

tuberoinfundibular peptide of 39 residues; cytoarchitectonic description; brainstem auditory nuclei; neuronal projection; retrograde and anterograde tracer; cholera toxin beta subunit

The paralemniscal region, a relatively little known area, is situated around the nuclei of the lateral lemniscus, in the lateral pontomesencephalic tegmentum (Andrezik and Beitz, 1985). Our interest in this region stems from the discovery of tuberoinfundibular peptide of 39 residues (TIP39; Usdin et al., 1999; Usdin, 2000). One of the two groups of neurons that synthesize TIP39 in the brain is situated in the paralemniscal region (Dobolyi et al., 2003b) medial to the



*Correspondence to: Arpád Dobolyi, Ph. D., Laboratory of Neuromorphology, Department of Anatomy, Histology and Embryology, Semmelweis University, Tüzolto u. 58, Budapest, H-1094, Hungary. dobolyi@ana.sote.hu..

intermediate nucleus of the lateral lemniscus as defined previously (Helfert and Aschoff, 1997; Schofield, 2005). Pharmacological and anatomical evidence suggests that TIP39 is the endogenous ligand of the parathyroid hormone 2 receptor (PTH2R). Initial functional studies suggest that TIP39 modulates nociceptive information processing (Dobolyi et al., 2002) and is involved in limbic (LaBuda et al., 2004; LaBuda and Usdin, 2004), reproductive (Dobolyi et al., 2006; Wang et al., 2006a), and endocrine regulation (Sugimura et al., 2003; Ward et al., 2001), and in the audiogenic stress response (Palkovits et al., 2004).

When we initially mapped the distribution of TIP39 cell bodies (Dobolyi et al., 2003b), we tentatively named the area of TIP39 expression immediately medial to the auditory relay nuclei of the lateral lemniscus the *medial paralemniscal nucleus* (MPL). However, the identification of this nucleus has not been straightforward without labeling TIP39. In the literature, often no distinction is made between oral reticular pontine and paralemniscal zones. Areas including cells that correspond to the MPL have been referred to by a great variety of anatomical names with poor topographical characterization, such as “lateral part of the nucleus reticularis pontis oralis” (Papez, 1926), “lateralmost nucleus reticularis pontis oralis” (Leichnetz et al., 1978), “ventrolateral tegmental area” (Herbert et al., 1997), or “dorsolateral pontomesencephalic reticular formation” (Haws et al., 1989). The term “paralemniscal” has also been used without detailed topographical characterization when describing an area in the “paralemniscal zone” whose stimulation elicited pinna movement in cats (Henkel and Edwards, 1978), a group of neurons whose activity changed in response to noxious stimuli in the “paralemniscal reticular formation” (Hardy et al., 1983), a group of neurons expressing Fos in response to suckling in the “caudal portion of the paralemniscal nucleus” (Li et al., 1999b), a group of audio-vocal neurons in the “paralemniscal tegmentum” (Metzner, 1993), and a group of neurons whose stimulation elicited vocalization in the “paralemniscal tegmental area” in bats (Schuller and Radtke-Schuller, 1990; Fenzl and Schuller, 2007), and the “ventral paralemniscal area” in squirrel monkey (Hage and Jurgens, 2006; Hannig and Jurgens, 2006).

Furthermore, the existence of a cell group probably corresponding to the MPL described in the present study was mentioned in early studies (Fuse, 1926; Wünscher et al., 1965), and also more recently as the “caudal part of the paralemniscal nucleus” (Andrezik and Beitz, 1985). However, the MPL is different from the paralemniscal nucleus described in a more rostral and lateral location (Taber, 1961; Olszewski and Baxter, 1982; Paxinos and Watson, 2005). The term “medial paralemniscal nucleus,” which was introduced recently (Dobolyi et al., 2003b), has been adopted by the widely used Paxinos rat brain atlas (Paxinos and Watson, 2005). In the last edition of this atlas (Paxinos and Watson, 2007), however, the term “medial ‘paralemniscial’ nucleus” was used, which might be incorrect grammatically.

Despite renewed interest in the MPL because of the expression of TIP39 in their neurons, it has not yet been cytoarchitectonically characterized, which hinders the comparison of its location with adjacent neuronal groups. In addition, we sought to determine the afferent neuronal connections of the MPL in order to distinguish it from nearby regions. An additional purpose was to provide information on the neuronal inputs to the MPL in order to facilitate the design of experiments aimed at elucidating the physiological role of neurons in the MPL including those that express TIP39. Therefore, in the present study we had the following objectives: 1) to describe the MPL cytoarchitectonically; 2) to examine afferent connections of the MPL and compare them with those of adjacent structures by injecting the retrograde tracer cholera toxin B subunit (CTB) into lemniscal and paralemniscal regions; and 3) to investigate projections of a major auditory and a major nonauditory site, which contained retrogradely labeled neurons following CTB injections into the MPL, toward the MPL by injecting the anterograde tracer biotinylated dextran amine into the auditory cortex and the hypothalamic ventromedial nucleus.

# MATERIALS AND METHODS

## Animals

A total of 56 adult male Wistar rats (250–300 g body weight; Charles River Laboratories, Budapest, Hungary) were used in this study. All efforts were made to minimize the number of animals used, and also their suffering. All procedures involving rats were carried out according to experimental protocols approved by the Animal Examination Ethical Council of the Animal Protection Advisory Board at the Semmelweis University, Budapest and meet the guidelines of the Animal Hygiene and Food Control Department, Ministry of Agriculture, Hungary. Animals were kept on standard laboratory conditions with 12-hour light/12-hour dark periods (lights on at 6.00 a.m.) and supplied with dry rat food and drinking water *ad libitum*. Rats were kept three per cage at a temperature of 22 ± 1°C. Rats were anaesthetized with an intramuscular injection of anesthetic mix containing 0.2 ml/300 g body weight ketamine (100 mg/ml) and 0.2 ml/300 g body weight xylazine (20 mg/ml) for tracer injections and perfusion.

## Tracer injections

The retrograde tracer CTB (List Biological Laboratories, Campbell, CA) was targeted to the medial paralemniscal nucleus (n = 29). Some of the misplaced injections were used as controls. In addition, we targeted the adjacent intermediate nucleus of the lateral lemniscus (n = 3) to obtain injections into this important control area. For stereotaxic injections, rats were positioned in a stereotaxic apparatus with the incisor bar set at –3.3 mm. Holes of about 2-mm diameter were drilled into the skull above the target coordinates. Glass micropipettes of 15–20-μm internal diameter were filled with 0.25% CTB dissolved in 0.1 M phosphate buffer at pH 7.4 (PB) and lowered to the targets of interest by using the following stereotaxic coordinates (Paxinos and Watson, 2005): AP = –8.3 mm from bregma, L = 2.4 mm from the midline, V = 6.8 mm from the surface of the dura mater for the medial paralemniscal nucleus, and AP = –8.3 mm, L = 3.1 mm, V = 6.8 mm for the intermediate nucleus of the lateral lemniscus. Once the pipette was in place, the CTB was injected by iontophoresis by using a constant current source (51413 Precision Current Source, Stoelting, Wood Dale, IL) that delivered a current of +6 μA, which pulsed for 7 seconds on and 7 seconds off for 15 minutes. Then the pipette was left in place for 10 minutes with no current and withdrawn under negative current. After tracer injections, the animals were allowed to survive for 7 days.

The anterograde tracer biotinylated dextran amine (BDA; 10,000 MW, Molecular Probes, Eugene, OR) was injected into layer V of the auditory cortex (n = 3) and the ventrolateral subdivision of the hypothalamic ventromedial nucleus (n = 3). The injections were carried out as for CTB, except that the glass micropipette was filled with 10% BDA. Furthermore, for auditory cortical injections, two injections were performed along the track of the micropipette to fill in different parts of a vertically elongated region of the primary auditory and ventral part of the secondary auditory cortices corresponding to temporal cortical areas 1 and 3 (Webster, 1977; Zilles and Wree, 1985; Roger and Arnault, 1989) that contained a high density of retrogradely labeled neurons. The coordinates were AP = –3.4 mm from bregma, L = 6.5 mm from the midline, V = 5.0 and 6.0 mm from the surface of the dura mater for the auditory cortex, and AP = –2.8 mm, L = 0.8, V = 9.4 mm for the hypothalamic ventromedial nucleus.

## Histology

**Tissue collection—**Rats were deeply anesthetized and perfused transcardially with 150 ml saline followed by 300 ml of ice-cold 4% paraformaldehyde in PB. Brains were removed and postfixed in the same fixative solution for 24 hours and transferred to PB containing 20% sucrose for 2 days. For side orientation on the sections, a small horizontal incision was made throughout the brains contralateral to the injection sites. Serial coronal sections were cut at 50 μm on a sliding microtome (SM 2000R, Leica Microsystems, Nussloch, Germany) from +4.0

to –14.0 mm of bregma levels for CTB-injected brains (n = 32) and –1.0 to –10.0 mm for BDA-injected brains (n = 6). In addition, serial coronal, sagittal, and horizontal sections were cut from 5-mm-thick blocks containing the medial paralemniscal nucleus. Each section from two sets of 6-6 coronal, sagittal, and horizontal blocks were used for cresyl-violet, and fluorescent Nissl stainings, as well as for double TIP39 and tyrosine hydroxylase (TH) immunocytochemistry. Sections were collected in PB containing 0.1% sodium azide and stored at 4°C until further processing.

**Cresyl-violet staining—**Sections were mounted consecutively on gelatin-coated slides and dried. Sections were stained in 0.1% cresyl-violet dissolved in PB and then differentiated in 96% ethanol containing acetic acid. Sections were then dehydrated and coverslipped with Cytoseal 60 (Stephens Scientific, Riverdale, NJ).

**Fluorescent Nissl staining combined with TIP39 immunolabeling—**Free-floating sections were immunolabeled first for TIP39, as described previously by using an affinity-purified polyclonal antiserum to TIP39 raised against rat TIP39 coupled to keyhole limpet hemocyanin by 1-ethyl-3-(3-dimethylaminopropyl) carbodiimide in rabbit. This antiserum labels cell bodies in rat with exactly the same distribution as observed by *in situ* hybridization histochemistry (Dobolyi et al., 2002, 2003a,b), and this staining can be preadsorbed by incubation of the diluted antiserum with 1 μM (4.5 μg/ml) of synthetic TIP39 (Dobolyi et al., 2002, 2003b).

Briefly, brain sections were pretreated in PB contaning 0.5% Triton X-100 and 3% bovine serum albumin for 1 hour. Then they were incubated with a primary antibody against TIP39 (1:2,500) in PB containing 0.5% Triton X-100, 3% bovine serum albumin, and 0.1% sodium azide for 48 hours at room temperature. Sections were then incubated in biotin-conjugated donkey anti-rabbit secondary antibody at 1:500 (Jackson ImmunoResearch, West Grove, PA) for 2 hours, followed by incubation in avidinbiotin-horseradish peroxidase complex (ABC) at 1:300 (Vectastain ABC Elite kit, Vector, Burlingame, CA) for 2 hours. Then sections were treated with fluorescein isothiocyanate (FITC)-tyramide (1:8,000) and 0.003% $H_2O_2$ in Tris-HCl buffer (0.05 M, pH 8.2) for 8 minutes, as described previously (Hunyady et al., 1996). After washing, the sections were incubated in Neurotrace red fluorescent Nissl stain (Molecular Probes) diluted to 1:30 for 2 hours, washed in PB overnight, mounted on positively charged slides (Superfrost Plus, Fisher Scientific, Fair Lawn, NJ), and coverslipped in antifade medium (Prolong Antifade Kit, Molecular Probes).

**Fluorescent Nissl staining combined with NeuN immunolabeling—**The double labeling was performed as described above for Neurotrace red fluorescent Nissl stain (Molecular Probes) and TIP39 except that the neuronal marker NeuN was labeled by using a mouse monoclonal anti-NeuN antibody (1:1,000; cat. #MAB377, lot #25070259, Chemicon, Temecula, CA). The immunogen for the production of this antibody was purified cell nuclei from mouse brain. This antibody recognizes the neuron-specific protein NeuN (Mullen et al., 1992), present in most central nervous system (CNS) and peripheral nervous system (PNS) neuronal cell types of all vertebrates tested (see manufacturer's technical data sheet for list of species). This antibody recognizes four bands on Western blot (Unal-Cevik et al., 2004) and is thought to reflect multiple phosphorylation states of NeuN (Lind et al., 2005). Application of the anti-NeuN antibody was followed by incubation in biotin-conjugated donkey anti-mouse secondary antibody at 1:500 (Jackson ImmunoResearch) for 2 hours.

**Double TIP39 and TH immunocytochemistry—**Free-floating sections were first immunolabeled for TIP39 by using FITC-tyramide amplification immunocytochemistry, as described above. Sections were incubated overnight in a mouse monoclonal anti-TH antibody (1:2000; cat. #MAB5280, clone name 2/40/15, lot #0607035618, Chemicon). For the

production of this antibody, the immunogen was purified TH from rat pheochromocytoma (see manufacturer's technical data sheet). This antibody provided the distribution of TH-immunoreactive neurons, which is well established in the literature (Hökfelt et al., 1976), including those located in the A7 noradrenaline cell group. After incubation in the primary antibody, sections were incubated in Alexa 594 donkey anti-mouse secondary antibody (1:500; Molecular Probes) for 2 hours and then mounted and coverslipped, as described above for fluorescent labeling.

**Visualization of CTB—**Every third brain section was stained for CTB by using an immunoperoxidase procedure. Free-floating sections were pretreated in PB containing 0.5% Triton X-100 and 3% bovine serum albumin for 1 hour. Sections were incubated in anti-CTB antiserum (1:30,000; product #703, lot #7032AA, List Biological Laboratories) at room temperature overnight. This antiserum was raised against CTB (choleragenid) in goat (see manufacturer's technical data sheet). The specificity of this antiserum was evident in our experiments by the dramatically different pattern of labeled cells depending on the injection sites, as described later. Following application of the primary antibody, sections were incubated in biotin-conjugated donkey anti-goat secondary antibody at 1:500 (Jackson ImmunoResearch) for 1 hour and then in ABC at 1:500 for 2 hours. Subsequently, the CTB-containing cells were visualized by incubation in 0.02% 3,3-diaminobenzidine (DAB; Sigma, St. Louis, MO), 0.08% nickel (II) sulfate, and 0.0012% hydrogen peroxide in PB for 4 minutes. Sections were mounted, and some of them were counterstained with 0.5% Kernechtrot solution, dehydrated, and coverslipped, as described above.

**Double labeling of CTB and TIP39—**Brain sections of animals injected with CTB were processed for double labeling with CTB and TIP39. Every third free-floating section was first stained for TIP39 by using FITC-tyramide amplification immunocytochemistry, as described above. Sections were then incubated overnight in goat anti-CTB antibody (1:30,000; List Biological Laboratories) at room temperature and then in Alexa 594 donkey anti-goat secondary antibody (1:500; Molecular Probes) for 2 hours. Sections were then mounted and coverslipped, as described above for fluorescent labeling.

**Visualization of BDA—**Sections from rat brains injected with BDA were stained for BDA by using immunoperoxidase labeling with biotin-tyramide amplification. Every third free-floating section was pretreated in PB containing 0.5% Triton X-100 for 1 hour and then incubated in ABC at 1:500 for 2 hours. Next, sections were placed in biotin-tyramide solution (1:1,000) containing 0.012% hydrogen peroxide for 20 minutes. Then, a second ABC incubation was conducted at 1:1,000 for 1 hour. Finally, the reaction product was visualized by incubation in 0.02% DAB, 0.08% nickel (II) sulfate, and 0.006% hydrogen peroxide in PB for 10 minutes. Sections were mounted, dehydrated and coverslipped, as described above.

**Double labeling of BDA and TIP39—**Brain sections of animals injected with BDA were processed for BDA-TIP39 double labeling. First, BDA visualization was performed followed by TIP39 immunolabeling. Every third section was pretreated in PB containing 0.5% Triton X-100 for 1 hour and then incubated in ABC (1:300) for 2 hours. Subsequently, BDA was visualized by using FITC-tyramide at 1:3,000 for 8 minutes. Following thorough rinses in PB, sections were then incubated with primary antibody against TIP39 (1:700) for 48 hours in PB containing 0.5% Triton X-100 and 3% bovine serum albumin. Subsequently, TIP39 was visualized by incubating the sections in Alexa Fluor 594 anti-rabbit secondary antibody (Molecular Probes) at 1:500 for 2 hours. Finally, sections were mounted and coverslipped, as described above for fluorescent labeling.

### Data analysis

Animals with CTB injection sites centered in the medial paralemniscal nucleus (n = 4), the intermediate nucleus of the lateral lemniscus, the rubrospinal tract, or the rostral and dorsal parts of the paralemniscal region, or located in the pontine reticular formation and other structures adjacent to the MPL (n = 12), as well as BDA injection sites centered in the ventrolateral subdivision of the hypothalamic ventromedial nucleus (n = 1) and the auditory cortex (n = 2) were included in the analysis for neuronal connections

Sections were examined by using an Olympus BX60 light microscope also equipped with fluorescent epi-illumination. Images were captured at 2,048 × 2,048 pixel resolution with a SPOT Xplorer digital CCD camera (Diagnostic Instruments, Sterling Heights, MI) by using 4–40× objectives.

Confocal images were acquired with a Nikon Eclipse E800 confocal microscope equipped with a BioRad Radiance 2100 Laser Scanninig System by using 20–40× objectives at optical thicknesses of 3–10 μm. The ratio of different cell types within the MPL was determined by using confocal photomicrographs of serial sections double labeled for TIP39 and a Neurotrace red fluorescent Nissl stain by analyzing 202 cells, in which the nucleolus was visible. The optical thickness of these confocal photomicrographs was 10 μm. For the calculation of the ratio of small vs. large cells in the medial paralemniscal nucleus, the Floderus correction was used (Floderus, 1944; Palkovits et al., 1971). This correction, calculated from the measurement of the average nucleolar radius and the smallest visible nucleolar calotte, compensates for the difference between measured and real cell number, which is necessary because the possibility of sectioning a large cell by the same section thickness is higher than that for a small cell. The sizes of the different cell types were determined by measuring the longest diameter (long axis) and the perpendicular small diameter of the cells.

Contrast and sharpness of the images were adjusted by using the levels and sharpness commands in Adobe Photoshop CS 8.0 (Adobe Systems, San Jose, CA). Full resolution was maintained until the photomicrographs were cropped and assembled for printing, at which point images were adjusted to a resolution of 300 dpi. Drawings were prepared by aligning the pictures with corresponding schematics adapted from a rat brain atlas (Paxinos and Watson, 2005).

## RESULTS

### Topography and cytoarchitecture of the medial paralemniscal nucleus

In coronal sections, cells of the MPL were distinguished from those in adjacent areas by their organization into dorsolaterally oriented cell columns evident in Nissl-stained (Figs. 1A, 2A) as well as NeuN-labeled sections (Fig. 2B). The cell columns were separated by 20–50-μm-wide cell-free zones, probably occupied by passing fibers of the lateral lemniscus. The ventral border of the MPL is the rubrospinal tract, which is easily distinguished and clearly separated by the abrupt end of the cell columns. However, lateral to the rubrospinal tract, the MPL extends somewhat ventrally (Figs. 1A, 2A,B). In addition, in the rostral half of the MPL, a small group of large cells is located between the medial part of the rubrospinal tract and the medial part of the MPL. Medially, the MPL borders on the oral part of the pontine reticular formation and the pedunculopontine tegmental nucleus, structures that do not exhibit columnar cytoarchitecture. The MPL narrows dorsally between the caudal part of the pedunculopontine tegmental nucleus and the dorsal nucleus of the lateral lemniscus, resulting in a cone shape of the nucleus (Figs. 1A, 2A,B). The lateral border of the MPL is the intermediate nucleus of the lateral lemniscus. Fiber bundles of the lateral lemniscus also pass through its own nuclei; however, the resulting columnar organization is not as pronounced as in the MPL.

Dorsoventrally oriented columnar cytoarchitecture of the MPL was also apparent in sagittal sections (Figs. 1B, 2C), suggesting that the MPL is formed by columns and not laminae. The MPL was clearly distinguished from the rostrally adjacent structures, the pedunculopontine tegmental nucleus medially, and the retrorubral nucleus and the paralemniscal nucleus laterally, as shown on sagittal (Fig. 1B, 2C) as well as horizontal sections (Figs. 1C, 2D). The cytoarchitecture of the MPL in horizontal sections was markedly different from that in coronal and sagittal sections. Cells did not appear aligned in columns in agreement with the dorsoventral orientation of the columnar structure of the nucleus (Figs. 1, 2). Instead, a grid-like arrangement of cells was visible, suggesting that the relative position of the cell columns was organized (Figs. 1C, 2D). Such a grid-like arrangement of cells was not apparent in adjacent structures in horizontal sections including the caudolaterally positioned Kölliker-Fuse nucleus and the caudomedially positioned area containing the A7 neurons, providing further evidence for a cytoarchitectonically distinct MPL (Figs. 1C, 2D).

Apart from the columnar organization of cells, three cell populations distinguishable by size and TIP39 content were also characteristic of the MPL. Small, slightly ovoid cells (average ± SEM: 12 ± 1 μm longest diameter (LD) and 9 ± 1 μm perpendicular small diameter (SD) on coronal, sagittal, and horizontal sections) were present throughout the MPL. These cells were not immunolabeled for TIP39 (Fig. 2A3,B3,C3) or NeuN (Fig. 2D3). These small cells amounted to 31% of the cells in the MPL. The large cells, which were all labeled for NeuN (Fig. 2D3) included a TIP39-positive and a TIP39-negative population (Fig. 2A3,B3,C3). On horizontal and sagittal sections, the sizes and the elongated shapes of TIP39-positive and -negative large cells did not differ (LD/SD: 25± 1/15 ± 1 μm). The orientation of the long axis was predominantly rostrocaudal and slightly mediolateral. In coronal sections, however, the TIP39-immunoreactive large cells (18 ± 1/12 ± 1 μm) were significantly smaller than the TIP39-negative large cells (22 ± 1/16 ± 1 μm). The TIP39-immunoreactive cells amounted to 75% of the large cells in the MPL, whereas the remaining 25% were TIP39-negative. Similar to the small cells, the TIP39-positive and the TIP39-negative large cells were evenly distributed within the MPL.

## Cells retrogradely labeled following CTB injection into the medial paralemniscal nucleus

Following CTB injections into the MPL, there was a relatively widespread distribution of CTB-labeled cells in the brain (Table 1). The topographical distribution of CTB-labeled cells following injections into the MPL was distinct from those observed following injections into adjacent brain regions including receipt of major inputs, e.g., from the auditory cortex and some hypothalamic structures. The majority of labeled cells were always ipsilateral to the injection side, with only a low or very low density of labeled cells present contralaterally. As discussed below, the periolivary area contains some of the most obvious labeling of contralateral cells. In some other regions that contained over 15 labeled cells ipsilaterally the number of labeled cells in the same regions contralaterally ranged from 0 to 5.

**Injection sites in the MPL—**TIP39-containing cell bodies occupied the MPL, as described above. The relation of the injection site to the position of TIP39 neurons was routinely verified by double labeling. There were four injections, in which the spread of tracer overlapped entirely or almost entirely with the location of the TIP39 neurons. The topographical distribution of CTB-labeled cells did not differ in these brains, and even the number of labeled cells in particular brain regions was very similar. Therefore, the description of the afferent connections of the MPL is based on the results of these four injections (Fig. 3). In addition, several different injections adjacent to the MPL resulted in labeling patterns markedly different from those following MPL injections. These injections were also included in the analysis of the afferent projections of the MPL as controls for MPL injections.

**Forebrain—**In the *cerebral cortex*, CTB-containing cells were restricted to particular regions. The most abundant labeling was in pyramidal cells of layer V in the ventral part of the secondary auditory cortex (Fig. 4B) in an area corresponding to cortical temporal area 3 (Te3), as defined previously (Webster, 1977;Zilles and Wree, 1985;Roger and Arnault, 1989). An almost equally high density of labeled pyramidal cells continued dorsally in the primary auditory cortex (Te1), whereas lower numbers of retrogradely labeled cells were found caudally in cortical temporal area 2 (Te2), ventrally in the ectorhinal and perirhinal cortices, and rostrally in the caudal part of the insular cortex (Figs. 4B, 5C–F). In addition, a few CTB-labeled cells were visible in layer VI of the ventral part of the auditory cortex, immediately adjacent to the external capsule. The number of labeled cells in layer VI increased in the ventral direction, with a high density of labeled cells visible in the perirhinal cortex (Figs. 4B, 5C–F).

Apart from the region of the auditory cortex, the somatosensory and somatomotor cortices also contained a significant number of retrogradely labeled neurons (Fig. 5A–E). Here, the labeled cells were restricted to pyramidal cells of layer V.

Additional forebrain structures including the *hippocampus*, *septum*, *basal ganglia*, and *basal forebrain* did not contain retrogradely labeled neurons (Fig. 5A–F). In turn, a small number of retrogradely labeled neurons were present in the *claustrum* (Fig. 4B) and the anterior cortical *amygdaloid* nucleus (Fig. 5B).

**Thalamus—**Most thalamic nuclei were not labeled with CTB following MPL injections. The posterior intralaminar complex of the thalamus (the subparafascicular area medially and the caudal paralaminar area laterally) was the only thalamic area that contained retrogradely labeled cells following MPL injections. Thus, the magnocellular and parvicellular subparafascicular nuclei as well as the surrounding periventricular gray, the posterior intralaminar and suprageniculate thalamic nuclei, the peripeduncular nucleus, and the medial nucleus of the medial geniculate body contained a high density of retrogradely labeled cells (Fig. 5E–H). It is interesting to note that the distribution of retrogradely labeled cells in the posterior intralaminar complex of the thalamus is similar to that of TIP39-immunoreactive neurons in the area. However, double labeling showed that the vast majority of cells projecting to the MPL were TIP39-negative (not shown).

**Hypothalamus—**The density of CTB-labeled cells was high in several regions of the hypothalamus (Fig. 5A–D). The ventromedial nucleus contained the greatest density of CTB-containing cells, particularly in its ventrolateral subdivison (Fig. 4D). A high density of retrogradely labeled neurons was also present in the lateral preoptic area, whereas the medial preoptic area contained only a few labeled cells (Fig. 4C). Different parts of the lateral hypothalamic area also contained a high density of retrogradely labeled cells. A cell group in the dorsolateral hypothalamic area, the area around the A13 catecholaminergic neurons, the lateral hypothalamic area next to the internal capsule, and the perifornical nucleus had a high density of CTB-labeled cells. In addition, a high density of retrogradely labeled cells was also present in the zona incerta.

**Midbrain—**Different areas of the midbrain contained a very high density of labeled cells after CTB injections into the MPL (Figs. 4E, 5F–J), including the periaqueductal gray, the inferior colliculus, and the cuneiform nucleus. In the periaqueductal gray, a particularly high density of labeled cells was present in the dorsomedial and lateral subdivisions throughout their rostrocaudal extent, whereas the dorsolateral and ventrolateral divisions contained a somewhat lower number of labeled cells (Figs. 4E, 5G–J). In the inferior colliculus, CTB-labeled cells were restricted to the external and dorsal cortices, whereas the central nucleus contained no retrogradely labeled cells (Figs. 4E, 5I–J). In addition, the deep mesencephalic nucleus, the nucleus of the brachium of the inferior colliculus, the precuneiform area, and the deep layers

of the superior colliculus also contained a high density of CTB cells following MPL injections, whereas in the medial and olivary pretectal nuclei, a moderate number of labeled cells were present (Fig. 5F–J). In contrast, the substantia nigra, the red nucleus, the oculomotor nuclei, and the interpeduncular nucleus did not contain CTB labeling (Fig. 5F–J).

**Pons—**In the pons, a high density of CTB-labeled cells following MPL injections was present in the contralateral MPL. Interestingly, the vast majority of these retrogradely labeled cells did not contain TIP39 immunoreactivity (not shown). Apart from the MPL, a moderate to high number of labeled cells was also present in the nucleus of the central acoustic tract, the superior paraolivary nucleus, and the periolivary area including the dorsal periolivary nucleus (Figs. 4E, 5I–J). In addition, the periolivary area contained a moderate number of retrogradely labeled cells contralaterally as well. Apart from the above mentioned sites, CTB-labeled cells were present, albeit only in low density, in the parabrachial nuclei and the magnocellular portion of the medial vestibular nucleus, whereas other regions in the pons including tegmental, pontine reticular, and pontine nuclei did not contain retrogradely labeled cells.

**Medulla oblongata and cerebellum—**The cerebellum and most parts of the medulla oblongata did not contain CTB-labeled cells following injection of the retrograde tracer in the MPL. However, a moderate density of labeled cells was present in the external part of the lateral paragigantocellular and spinal trigeminal nuclei. Furthermore, the intermediate reticular nucleus contained a moderate number of labeled cells contralateral to the injection site.

### Retrogradely labeled cell bodies following CTB injections into regions adjacent to the medial paralemniscal nucleus

Several different injections adjacent to the MPL and indicated in Figure 4 were analyzed as controls. For example, injection of CTB immediately dorsal to the MPL (Fig. 6A; injection site 22 in Fig. 3) resulted in significant retrograde labeling in the ipsilateral periaqueductal gray, particularly its dorsolateral subdivision (Fig. 6B), deep layers of the superior colliculus (Fig. 6B), the supraoptic decussations, the peripeduncular area, and the external cortex of the inferior colliculus but not in any other brain regions that project to the MPL including the auditory cortex where only a few labeled cells were found probably resulting from the spread of a small amount of tracer into the MPL (Fig. 6C). Furthermore, injection into the intermediate nucleus of the lateral lemniscus lateral to the MPL (Fig. 6D, injection site 14 in Fig. 3) resulted in significant retrograde labeling in the contralateral ventral cochlear nuclei (Fig. 6E), and in the ipsilateral superior olive but in none of the brain regions that project to the MPL including the auditory cortex (Fig. 6F). Injection of CTB immediately dorsomedial to the MPL (injection sites 17 and 23 in Fig. 3) resulted in ipsilateral retrograde labeling in the insular cortex, the bed nucleus of the stria terminalis, the central amygdaloid nucleus, lateral preoptic and hypothalamic areas, the hypothalamic paraventricular nucleus, the periaqueductal gray, and the nucleus of the solitary tract but not in any other brain regions that project to the MPL. Injection of CTB ventral to the MPL in the rubrospinal tract (injection site 7 in Fig. 3) resulted in moderate retrograde labeling in the ipsilateral periaqueductal gray and the contralateral red nucleus, suggesting some uptake by descending fibers but no labeling in other brain regions that project to the MPL. In general, non-overlapping control injections resulted in labeling patterns markedly different from those following MPL injections.

### Anterogradely labeled fibers in the MPL following BDA injections into the hypothalamic ventromedial nucleus and the auditory cortex

We chose the hypothalamic ventromedial nucleus and the auditory cortex to confirm the results obtained by using a retrograde tracer because these brain areas contained a very high number of retrogradely labeled cells, suggesting surprisingly massive projections to the MPL. These

projections are also intriguing because they represent potential inputs from different regulatory systems toward the MPL.

Following injection of the anterograde tracer BDA into the ventrolateral subdivision of the hypothalamic ventromedial nucleus (Fig. 7A), a large number of labeled fibers appeared in different brain regions, including, for example, the medial hypothalamus, the amygdala, and the periaqueductal gray, in agreement with previous studies (Canteras et al., 1994). Significant numbers of anterogradely labeled fibers were also present in the MPL with ipsilateral predominance (Fig. 7B). Fibers and fiber terminals were evenly distributed within the MPL, but they were not present in adjacent nuclei (Fig. 7B). The presence of terminals of the BDA fibers was apparent on high-magnification images (Fig. 7C).

Following injection of BDA into the primary and secondary auditory cortices (Fig. 7D), labeled fibers appeared in different brain regions including the contralateral auditory cortex, the medial geniculate body, and the inferior colliculus, in agreement with previous studies (Roger and Arnault, 1989;Arnault and Roger, 1990). Significant numbers of anterogradely labeled fibers and fiber terminals were also present in the ipsilateral MPL but not in adjacent nuclei (Fig. 7E). The anterogradely labeled fibers were distributed evenly within the MPL (Fig. 7E). The presence of terminals of the BDA fibers was apparent on high-magnification images (Fig. 7F).

## DISCUSSION

This study shows that the MPL is distinct from the surrounding brain regions. In this discussion, we define the MPL cytoarchitectonically as well as neurochemically. We also discuss the afferent connections of the MPL in relation to the literature, and the potential functional significance of the projections to the MPL.

### The medial paralemniscal nucleus

The MPL has a characteristic cytoarchitecture resulting from the dorsoventrally oriented columnar arrangement of its cells. Morphologically, we were able to distinguish three cell populations within the nucleus, indicating that the MPL consists of heterogeneous cell populations. The NeuN-negative cells are likely to be glial cells amounting to about one-third of the cells in the MPL. Most of the neuronal cell population (75%) expresses TIP39, making TIP39 neurons the largest cell group in the MPL. Apart from the expression of TIP39, TIP39-positive and -negative neurons may have different functional characteristics. We have demonstrated that only TIP39-negative paralemniscal neurons project to the contralateral MPL, indicating a different projection pattern of the two types of neurons. The distributions of the three cell populations overlap entirely, and all of them participate in the formation of cell columns within the MPL. It is plausible that this cellular arrangement is an inherent property of MPL; alternatively, it might be due to the organization of the abundant tracts and fiber bundles passing through the MPL and hence might differ in different species.

The cone-shaped structure of the MPL can be cytoarchitectonically distinguished from adjacent brain regions in the lateral pontomesencephalic tegmentum based on the columnar arrangement of its neurons, suggesting that it is a distinct nucleus. The rostral part of the MPL is embedded between the pedunculopontine tegmental and the retrorubral nuclei from which the MPL is separated by a zone of lower cell density. The dorsolateral and lateral borders of the MPL are the dorsal and intermediate nuclei of the lateral lemniscus, respectively. Medially, the MPL borders the oral part of the pontine reticular formation, which contains cells of markedly different morphology from those in the MPL. In turn, the caudal borders of the MPL are the Kölliker-Fuse nucleus laterally and the region of the A7 cell group medially. Ventrally, the MPL lies on the rubrospinal tract except for the medial part of its rostral half, where large

acetylcholinesterase-positive cells of the epirubrospinal nucleus surround the rubrospinal tract (Paxinos and Butcher, 1985).

Apart from the cytoarchitectonic differences, a distinct MPL is also supported by our finding that the afferent connections of the MPL differ markedly from those of adjacent brainstem nuclei. The lack of previous description of the MPL probably stems from the difficulty in defining the area functionally and even topographically without neurochemical markers, which may have contributed to the usage of different terminologies describing overlapping parts of the paralemniscal region, as detailed in the Introduction. However, as far as we could judge, only the area where neurons express Fos protein in response to suckling stimulus (Li et al., 1999b) corresponds perfectly to the MPL.

### Neuronal inputs to the medial paralemniscal nucleus

Labeled cells following CTB injections into the MPL represent cells that project to the MPL (Lencer and Tsai, 2003). Neurons projecting to brain structures adjacent to the MPL are not likely to contribute to retrogradely labeled cells following MPL injections because markedly different patterns of labeled cells were seen after injections of tracers into adjacent nuclei. In fact, fibers and fiber terminals arising from the auditory cortex and the hypothalamic ventromedial nucleus that entered the lateral pontomesencephalic tegmentum were largely confined to the MPL, confirming the results of CTB injections. The uptake of the tracer by passing fibers in the MPL is also not likely to contribute to retrogradely labeled cells because the origins of major fiber tracts in and around the MPL, the cochlear and superior olivary nuclei for the lateral lemniscus and the red nucleus for the rubrospinal tract, were largely devoid of labeling.

The MPL receives neuronal inputs from brain areas associated with auditory information processing including the auditory cortex, the posterior intralaminar complex of the thalamus, the deep layers of the superior colliculus, the inferior colliculus, and the periolivary area (Fig. 8). In addition, the MPL receives neuronal inputs from brain areas not known to be involved primarily in auditory processing, such as the lateral preoptic area, the hypothalamic ventromedial nucleus, parts of the lateral and dorsal hypothalamic areas, the zona incerta, the periaqueductal gray, and the deep mesencephalic and cuneiform nuclei (Fig. 8). These afferent connections of the MPL differ from the afferent connections of paralemniscal regions described in previous studies such as the paralemniscal reticular formation (Hardy et al., 1983), and the vocalization centers in squirrel monkey (Hannig and Jürgens, 2005). In turn, the afferent connections of the MPL are somewhat similar to a site in the “lateral midbrain tegmental zone,” which has been suggested to be involved in pinnae movement (Henkel, 1981), and the paralemniscal vocalization center in the “paralemniscal tegmentum” in bats (Metzner, 1996). Nevertheless, the cerebral cortical, intralaminar thalamic, and hypothalamic inputs differentiate the MPL from these sites as well.

Our data are consistent, however, with reports of some previous anterograde studies. Although the MPL was not recognized in a study of the efferent connections of the hypothalamic ventromedial nucleus, the drawings clearly indicate fibers and fiber terminals of hypothalamic ventromedial origin in the area corresponding to the MPL (Canteras et al., 1994). Similarly, a recent study on auditory cortical-pontine projections in cat indicates a high density of anterogradely labeled fibers in the area corresponding to the MPL following injection of anterograde tracer in the auditory cortex (Perales et al., 2006).

### Possible functions of neurons in the medial paralemniscal nucleus

Few functional data are available regarding the MPL. The paralemniscal vocalization center of bats occupies a similar position medial to the intermediate nucleus of the lateral lemniscus.

However, the bat vocalization center has partially different afferent connections, including, for example, the superior olive and the dorsal nucleus of the lemniscus lateralis (Metzner, 1996). Because of these discrepancies, it is difficult to suggest that the MPL has a function related to vocalization in rats. Similarly, it is not apparent from the available data whether the MPL plays a role in the pinnae movement, which involves a paralemniscal site in cats. Both of these functions require projections toward the motor facial nucleus. Currently, we do not have a complete understanding of the efferent projections of the medial paralemniscal neurons. However, TIP39 fibers are not present in the motor facial nucleus (Dobolyi et al., 2003b), suggesting that paralemniscal TIP39 neurons do not project there.

Based on its neuronal connections, the MPL seems to be intimately involved with the external cortex of the inferior colliculus, suggesting that they are involved in overlapping functions. In the present study we showed that the MPL receives major input from the external cortex of the inferior colliculus. In addition, in a previous lesion study, we demonstrated that the particularly dense network of TIP39 fibers in the external cortex of the inferior colliculus (Dobolyi et al., 2003b) originates in the MPL (Dobolyi et al., 2003a). Therefore, as opposed to the auditory cortex or the hypothalamic ventromedial nucleus, which do not contain TIP39 fibers, the external cortex of the inferior colliculus is massively interconnected with the MPL. We also demonstrated that the MPL, similar to the external cortex of the inferior colliculus (Herbert et al., 1991; Winer et al., 1998), receives massive inputs from primary and secondary auditory cortices. The massive corticocollicular pathway has been demonstrated to play a part in the induction of Fos in the external cortex of the inferior colliculus (Burow et al., 2005; Sun et al., 2007). We have previously demonstrated *c-fos* activation in the MPL in response to loud noise (Palkovits et al., 2004) possibly resulting from the cortical and collicular inputs described. As opposed to the central nucleus, neurons of the external cortex of the inferior colliculus do not receive significant input from brainstem auditory relay nuclei other than the central nucleus of the inferior colliculus itself (Faye-Lund and Osen, 1985; Saldaña and Merchn, 2005), and their activity is not tonotopically organized (Clopton et al., 1974).

In turn, it has been suggested that neurons of the external cortex of the inferior colliculus are sites for integration of auditory and somatosensory information (Zhou and Shore, 2006). Neurons there may play a part in the modulation of vigilance and attention by auditory stimuli (Jane et al., 1965) and may mediate cortical input on filtering (Bregman, 1990), e.g., based on the global location of a sound in space (Middlebrooks et al., 1994). In addition, they may regulate orientation behaviors, e.g., head and pinna movement and audio-vocal interfaces (Thompson, 1997), provide information to a map of auditory space (King et al., 1998) and to the coordination of responses to sound (Schuller et al., 1991), function as novelty detector neurons (Perez-Gonzalez et al., 2005), and modulate the acoustic startle response (Yeomans et al., 2002).

Based on its neuronal connections, the MPL's functions also seem to be related to that of the posterior intralaminar complex of the thalamus, as defined previously (Ledoux et al., 1987). The MPL receives input from the medially positioned subparafascicular area and the laterally positioned caudal paralaminar area as well. Similarly to the MPL, both of these regions of the posterior intralaminar complex of the thalamus contain TIP39 neurons (Dobolyi et al., 2003b). Interestingly, however, predominantly TIP39-negative neurons project to the MPL. This relationship is similar to our previous finding that TIP39-negative neurons of the MPL project to the subparafascicular area (Wang et al., 2006b). A further connection between the posterior intralaminar thalamic complex and the MPL is the massive input from the hypothalamic ventromedial nucleus and the inferior colliculus (Ledoux et al., 1987; Coolen et al., 2003; Wang et al., 2006b). The posterior intralaminar complex of the thalamus has been suggested to process auditory inputs to emotional brain centers (LeDoux et al., 1990). Furthermore, stimulation (Shimura and Shimokochi, 1991), lesion (Maillard and Edwards,

1991), and activation studies (Coolen et al., 1997; Holstege et al., 2003) have implicated the subparafascicular area in sexual functions. In particular, TIP39 neurons have been shown to be activated following male sexual behavior (Wang et al., 2006a).

Based on its input from reproductive brain centers (Sachs and Meisel, 1988; Numan and Sheehan, 1997; Simerly, 2002) including the subparafascicular area, the lateral preoptic area, the estrogen receptor-expressing ventrolateral subdivision of the hypothalamic ventromedial nucleus (Lauber et al., 1991; Shughrue et al., 1997), and the periaqueductal gray, the MPL might also play a role in some reproductive behaviors. In fact, *c-fos* activation has been reported in the "caudal portion of the paralemniscal nucleus" immediately dorsolateral to the A7 cell group following suckling stimulus (Li et al., 1999b). The activated neurons have been suggested to exert an action on lactation via their projections to the arcuate nucleus (Li et al., 1999a). The paralemniscal region has also been implicated in brainstem pain-regulatory systems based on changes in the activity of its neurons in response to noxious stimuli (Hardy et al., 1983) and analgesic effects of its stimulation (Haws et al., 1989; Zhao and Duggan, 1988). Because TIP39 affected nociceptive information transmission (Dobolyi et al., 2002) and pain-related affective behaviors (LaBuda and Usdin, 2004), it is possible that TIP39 neurons in the MPL contribute to these actions.

*In conclusion*, we have provided a cytoarchitectonic identification of the medial paralemniscal nucleus in the lateral pontomesencephalic tegmentum of the rat. This nucleus contains the newly identified neuropeptide TIP39. We have also described the afferent neuronal connections of the medial paralemniscal nucleus, which suggests major auditory and hypothalamic inputs to the nucleus.

## ACKNOWLEDGMENTS

We are grateful for the technical assistance of Erzsébet Tárnokné Vörös and Dorottya Kézdi.

Grant sponsor: the Hungarian Science Foundation; Grant numbers: NKTH-OTKA K67646 (to A.D.) and OTKA TS49861 (to M.P.); Grant sponsor: the National Institute of Mental Health Intramural Research Program (to T.B.U.); Grant sponsor: the Bolyai János Scholarship (to A.D.).

## Abbreviations

ACo, anterior cortical amygdaloid nucleus
Aq, cerebral aqueduct
AudCx, auditory cortex
AuV, ventral part of the secondary auditory cortex
Au1, primary auditory cortex
A7, A7 noradrenergic cell group
A13, A13 dopaminergic cell group
BIC, nucleus of the brachium of the inferior colliculus
BNST, bed nucleus of the stria terminalis
cc, corpus callosum
Cl, claustrum
CnF, cuneiform nucleus
CP, caudate putamen
DLL, dorsal nucleus of the lateral lemniscus
DLPAG, dorsolateral division of the periaqueductal gray
DpMe, deep mesencephalic nucleus
ECIC, external cortex of the inferior colliculus
EGP, external globus pallidus
f, fornix

ic, internal capsule
IC, inferior colliculus
IPAC, posterior interstitial nucleus of the anterior commissure
JPLH, juxtaparaventricular lateral hypothalamic area
LH, lateral hypothalamic area
ILL, intermediate nucleus of the lateral lemniscus
KF, Kölliker-Fuse nucleus
LH, lateral hypothalamic area
LPGi, lateral paragigantocellular nucleus
LPO, lateral preoptic area
LV, lateral ventricle
mcp, medial cerebellar peduncle
MG, medial geniculate body
MGM, medial nucleus of the medial geniculate body
MPA, medial preoptic area
MPL, medial paralemniscal nucleus
MPT, medial pretectal nucleus
mSPF, magnocellular subparafascicular nucleus
mt, mamillothalamic tract
MVe, medial vestibular nucleus
MVeMC, magnocellular part of the medial vestibular nucleus
M1, primary somatomotor cortex
M5, motor trigeminal nucleus
ot, optic tract
PA, periolivary area
PAG, periaqueductal gray
PIL, posterior intralaminar thalamic nucleus
PL, paralemniscal nucleus
PnO, pontine reticular nucleus, oral part
PP, peripeduncular nucleus
PPTg, pedunculopontine tegmental nucleus
PrCnF, precuneiform area
PRh, perirhinal cortex
PVN, paraventricular nucleus of the hypothalamus
py, pyramidal tract
RR, retrorubral nucleus
rs, rubrospinal tract
SC, superior colliculus
scp, superior cerebellar peduncle
SG, suprageniculate thalamic nucleus
SN, substantia nigra
SOC, superior olivary complex
SPF, subparafascicular area
Sp5, spinal trigeminal nucleus
Sp5O, spinal trigeminal nucleus, oral part
S1, primary somatosensory cortex
TIP39, tuberoinfundibular peptide of 39 residues
VCA, ventral cochlear nucleus, anterior subdivision
VLL, ventral nucleus of the lateral lemniscus
VMH, hypothalamic ventromedial nucleus
ZI, zona incerta
3V, third ventricle
4V, fourth ventricle

7n, facial nerve

## LITERATURE CITED


Andrezik, JE.; Beitz, AJ. Reticular formation, central gray and related tegmental nuclei.. In: Paxinos, G., editor. The rat nervous system. Academic Press; New York: 1985. p. 1-28.

Arnault P, Roger M. Ventral temporal cortex in the rat: connections of secondary auditory areas te2 and te3. J Comp Neurol 1990;302:110–123. [PubMed: 1707895]

Bregman, AS. The perceptual organization of sound. MIT Press; Cambridge: 1990. Auditory scene analysis..

Burow A, Day HE, Campeau S. A detailed characterization of loud noise stress: intensity analysis of hypothalamo-pituitary-adrenocortical axis and brain activation. Brain Res 2005;1062:63–73. [PubMed: 16256084]

Canteras NS, Simerly RB, Swanson LW. Organization of projections from the ventromedial nucleus of the hypothalamus: a *Phaseolus vulgaris*-leucoagglutinin study in the rat. J Comp Neurol 1994;348:41–79. [PubMed: 7814684]

Clopton BM, Winfield JA, Flammino FJ. Tonotopic organization: review and analysis. Brain Res 1974;76:1–20. [PubMed: 4367399]

Coolen LM, Peters HJ, Veening JG. Distribution of fos immunoreactivity following mating versus anogenital investigation in the male rat brain. Neuroscience 1997;77:1151–1161. [PubMed: 9130794]

Coolen LM, Veening JG, Wells AB, Shipley MT. Afferent connections of the parvocellular subparafascicular thalamic nucleus in the rat: evidence for functional subdivisions. J Comp Neurol 2003;463:132–156. [PubMed: 12815752]

Dobolyi A, Ueda H, Uchida H, Palkovits M, Usdin TB. Anatomical and physiological evidence for involvement of tuberoinfundibular peptide of 39 residues in nociception. Proc Natl Acad Sci U S A 2002;99:1651–1656. [PubMed: 11818570]

Dobolyi A, Palkovits M, Bodnar I, Usdin TB. Neurons containing tuberoinfundibular peptide of 39 residues project to limbic, endocrine, auditory and spinal areas in rat. Neuroscience 2003a;122:1093–1105. [PubMed: 14643775]

Dobolyi A, Palkovits M, Usdin TB. Expression and distribution of tuberoinfundibular peptide of 39 residues in the rat central nervous system. J Comp Neurol 2003b;455:547–566. [PubMed: 12508326]

Dobolyi A, Wang J, Irwin S, Usdin TB. Postnatal development and gender-dependent expression of tip39 in the rat brain. J Comp Neurol 2006;498:375–389. [PubMed: 16871538]

Faye-Lund H, Osen KK. Anatomy of the inferior colliculus in rat. Anat Embryol (Berl) 1985;171:1–20. [PubMed: 3985354]

Fenzl T, Schuller G. Dissimilarities in the vocal control over communication and echolocation calls in bats. Behav Brain Res 2007;182:173–179. [PubMed: 17227683]

Floderus S. Untersuchungen über den bau der menschlichen hypophyse mit besonderer berücksichtigung der quantitativen mikromorphologische verhaltnisse. Acta Pathol Microbiol Scand Suppl 1944;53:276.

Fuse G. Vergleichend-anatomische beobachtungen am hirnstamme der saugetiere. Viii.: Eine weitere bemerkung über den nucleus ventralis accessorius lemnisci lateralis bei einigen karnivoren (katze, hund, fuchs, dachs, meler anakuma). Arb Anat Inst Sendai 1926;12:39–44.

Hage SR, Jurgens U. On the role of the pontine brainstem in vocal pattern generation: a telemetric single-unit recording study in the squirrel monkey. J Neurosci 2006;26:7105–7115. [PubMed: 16807339]

Hannig S, Jurgens U. Projections of the ventrolateral pontine vocalization area in the squirrel monkey. Exp Brain Res 2006;169:92–105. [PubMed: 16292643]

Hardy SG, Haigler HJ, Leichnetz GR. Paralemniscal reticular formation: response of cells to a noxious stimulus. Brain Res 1983;267:217–223. [PubMed: 6307465]

Haws CM, Williamson AM, Fields HL. Putative nociceptive modulatory neurons in the dorsolateral pontomesencephalic reticular formation. Brain Res 1989;483:272–282. [PubMed: 2706520]

Helfert, RH.; Aschoff, A. Superior olivary complex and nuclei of the lateral lemniscus.. In: Ehret, G.; Raymond, R., editors. The central auditory system. Oxford University Press; Oxford: 1997. p. 233

Henkel CK. Afferent sources of a lateral mdibrain tegmental zone associated with the pinnae in the cat as mapped by retrograde transport of horseradish peroxide. J Comp Neurol 1981;203:213–226. [PubMed: 7309921]

Henkel CK, Edwards SB. The superior colliculus control of pinna movements in the cat: possible anatomical connections. J Comp Neurol 1978;182:763–776. [PubMed: 730846]

Herbert H, Aschoff A, Ostwald J. Topography of projections from the auditory cortex to the inferior colliculus in the rat. J Comp Neurol 1991;304:103–122. [PubMed: 2016407]

Herbert H, Klepper A, Ostwald J. Afferent and efferent connections of the ventrolateral tegmental area in the rat. Anat Embryol (Berl) 1997;196:235–259. [PubMed: 9310315]

Hökfelt T, Johansson O, Fuxe K, Goldstein M, Park D. Immunohistochemical studies on the localization and distribution of monoamine neuron systems in the rat brain. I. Tyrosine hydroxylase in the mesand diencephalon. Med Biol 1976;54:427–453. [PubMed: 12423]

Holstege G, Georgiadis JR, Paans AM, Meiners LC, van der Graaf FH, Reinders AA. Brain activation during human male ejaculation. J Neurosci 2003;23:9185–9193. [PubMed: 14534252]

Hunyady B, Krempels K, Harta G, Mezey E. Immunohistochemical signal amplification by catalyzed reporter deposition and its application in double immunostaining. J Histochem Cytochem 1996;44:1353–1362. [PubMed: 8985127]

Jane JA, Masterton RB, Diamond IT. The function of the tectum for attention to auditory stimuli in the cat. J Comp Neurol 1965;125:165–191. [PubMed: 5852848]

King AJ, Jiang ZD, Moore DR. Auditory brainstem projections to the ferret superior colliculus: Anatomical contribution to the neural coding of sound azimuth. J Comp Neurol 1998;390:342–365. [PubMed: 9455897]

LaBuda CJ, Usdin TB. Tuberoinfundibular peptide of 39 residues decreases pain-related affective behavior. Neuroreport 2004;15:1779–1782. [PubMed: 15257146]

LaBuda CJ, Dobolyi A, Usdin TB. Tuberoinfundibular peptide of 39 residues produces anxiolytic and antidepressant actions. Neuroreport 2004;15:881–885. [PubMed: 15073536]

Lauber AH, Mobbs CV, Muramatsu M, Pfaff DW. Estrogen receptor messenger RNA expression in rat hypothalamus as a function of genetic sex and estrogen dose. Endocrinology 1991;129:3180–3186. [PubMed: 1954897]

Ledoux JE, Ruggiero DA, Forest R, Stornetta R, Reis DJ. Topographic organization of convergent projections to the thalamus from the inferior colliculus and spinal cord in the rat. J Comp Neurol 1987;264:123–146. [PubMed: 2445791]

LeDoux JE, Farb C, Ruggiero DA. Topographic organization of neurons in the acoustic thalamus that project to the amygdala. J Neurosci 1990;10:1043–1054. [PubMed: 2158523]

Leichnetz GR, Watkins L, Griffin G, Murfin I, Mayer DJ. The projection from the nucleus raphe magnus and other brainstem nuclei to the spinal cord in the rat: a study using the HRP blue-reaction. Neurosci Lett 1978;8:119–124.

Lencer WI, Tsai B. The intracellular voyage of cholera toxin: going retro. Trends Biochem Sci 2003;28:639–645. [PubMed: 14659695]

Li C, Chen P, Smith MS. Identification of neuronal input to the arcuate nucleus (ARH) activated during lactation: implications in the activation of neuropeptide Y neurons. Brain Res 1999a;824:267–276. [PubMed: 10196458]

Li C, Chen P, Smith MS. Neural populations in the rat forebrain and brainstem activated by the suckling stimulus as demonstrated by cfos expression. Neuroscience 1999b;94:117–129. [PubMed: 10613502]

Lind D, Franken S, Kappler J, Jankowski J, Schilling K. Characterization of the neuronal marker NeuN as a multiply phosphorylated antigen with discrete subcellular localization. J Neurosci Res 2005;79:295–302. [PubMed: 15605376]

Maillard CA, Edwards DA. Excitotoxin lesions of the zona incerta/lateral tegmentum continuum: effects on male sexual behavior in rats. Behav Brain Res 1991;46:143–149. [PubMed: 1664729]

Metzner W. An audio-vocal interface in echolocating horseshoe bats. J Neurosci 1993;13:1899–1915. [PubMed: 8478683]

Metzner W. Anatomical basis for audio vocal integration in echolocating horseshoe bats. J Comp Neurol 1996;368:252–269. [PubMed: 8725305]

Middlebrooks JC, Clock AE, Xu L, Green DM. A panoramic code for sound location by cortical neurons. Science 1994;264:842–844. [PubMed: 8171339]

Mullen RJ, Buck CR, Smith AM. NeuN, a neuronal specific nuclear protein in vertebrates. Development 1992;116:201–211. [PubMed: 1483388]

Numan M, Sheehan TP. Neuroanatomical circuitry for mammalian maternal behavior. Ann N Y Acad Sci 1997;807:101–125. [PubMed: 9071346]

Olszewski, J.; Baxter, D. Cytoarchitecture of the human brain stem. Karger; New York: 1982.

Palkovits M, Magyar P, Szentgothai J. Quantitative histological analysis of the cerebellar cortex in the cat: I. Number and arrangement in space of the Purkinje cells. Brain Res 1971;32:1–13. [PubMed: 4107040]

Palkovits M, Dobolyi A, Helfferich F, Usdin TB. Localization and chemical characterization of the audiogenic stress pathway. Ann N Y Acad Sci 2004;1018:16–24. [PubMed: 15240348]

Papez JW. Reticulo-spinal tracts in the cat. Marchi method. J Comp Neurol 1926;41:365–399.

Paxinos, G.; Butcher, LL. Organizational principles of the brain as revealed by choline acetyltransferase and acetylcholinesterase distribution and projections.. In: Paxinos, G., editor. The rat nervous system. Academic Press; Sydney: 1985. p. 487-521.

Paxinos, G.; Watson, C. The rat brain in stereotaxic coordinates. Academic Press; San Diego: 1998.

Paxinos, G.; Watson, C. The rat brain in stereotaxic coordinates. Academic Press; San Diego: 2005.

Paxinos, G.; Watson, C. The rat brain in stereotaxic coordinates. Academic Press; San Diego: 2007.

Perales M, Winer JA, Prieto JJ. Focal projections of cat auditory cortex to the pontine nuclei. J Comp Neurol 2006;497:959–980. [PubMed: 16802335]

Perez-Gonzalez D, Malmierca MS, Covey E. Novelty detector neurons in the mammalian auditory midbrain. Eur J Neurosci 2005;22:2879–2885. [PubMed: 16324123]

Roger M, Arnault P. Anatomical study of the connections of the primary auditory area in the rat. J Comp Neurol 1989;287:339–356. [PubMed: 2778109]

Sachs, BD.; Meisel, RL. The physiology of male sexual behavior.. In: Knobil, E.; Meill, J., editors. The physiology of reproduction. Raven Press; New York: 1988.

Saldaña, E.; Merín, MA. Intrinsic and commissural connections of the inferior colliculus.. In: Winer, JA.; Schreiner, CE., editors. The inferior colliculus. Springer-Verlag; New York: 2005. p. 155-181.

Schofield, BR. Superior olivary complex and lateral lemniscal connections of the auditory midbrain.. In: Winer, JA.; Schreiner, CE., editors. The inferior colliculus. Springer-Verlag; New York: 2005. p. 133-154.

Schuller G, Radtke-Schuller S. Neural control of vocalization in bats: mapping of brainstem areas with electrical microstimulation eliciting species-specific echolocation calls in the rufous horseshoe bat. Exp Brain Res 1990;79:192–206. [PubMed: 2311697]

Schuller G, Covey E, Casseday JH. Auditory pontine grey: connections and response properties in the horseshoe bat. Eur J Neurosci 1991;3:648–662. [PubMed: 12106473]

Shimura T, Shimokochi M. Modification of male rat copulatory behavior by lateral midbrain stimulation. Physiol Behav 1991;50:989–994. [PubMed: 1805289]

Shughrue PJ, Lane MV, Merchenthaler I. Comparative distribution of estrogen receptor-alpha and -beta mRNA in the rat central nervous system. J Comp Neurol 1997;388:507–525. [PubMed: 9388012]

Simerly RB. Wired for reproduction: organization and development of sexually dimorphic circuits in the mammalian forebrain. Annu Rev Neurosci 2002;25:507–536. [PubMed: 12052919]

Sugimura Y, Murase T, Ishizaki S, Tachikawa K, Arima H, Miura Y, Usdin TB, Oiso Y. Centrally administered tuberoinfundibular peptide of 39 residues inhibits arginine vasopressin release in conscious rats. Endocrinology 2003;144:2791–2796. [PubMed: 12810532]

Sun X, Xia Q, Lai CH, Shum DK, Chan YS, He J. Corticofugal modulation of acoustically induced fos expression in the rat auditory pathway. J Comp Neurol 2007;501:509–525. [PubMed: 17278128]

Taber E. The cytoarchitecture of the brain stem of the cat. I. Brain stem nuclei of cat. J Comp Neurol 1961;116:27–69. [PubMed: 13774738]

Thompson, AM. Descending connections of the auditory midbrain.. In: Ehret, G.; Romand, R., editors. The central auditory system. Oxford University Press; Oxford: 1997. p. 182-199.

Unal-Cevik I, Kilinc M, Gursoy-Ozdemir Y, Gurer G, Dalkara T. Loss of NeuN immunoreactivity after cerebral ischemia does not indicate neuronal cell loss: a cautionary note. Brain Res 2004;1015:169–174. [PubMed: 15223381]

Usdin TB. The pth2 receptor and tip39: a new peptide-receptor system. Trends Pharmacol Sci 2000;21:128–130. [PubMed: 10740285]

Usdin TB, Hoare SR, Wang T, Mezey E, Kowalak JA. Tip39: a new neuropeptide and pth2-receptor agonist from hypothalamus. Nat Neurosci 1999;2:941–943. [PubMed: 10526330]

Wang J, Coolen LM, Brown JL, Usdin TB. Neurons containing tuberoinfundibular peptide of 39 residues are activated following male sexual behavior. Neuropeptides. 2006a

Wang J, Palkovits M, Usdin TB, Dobolyi A. Afferent connections of the subparafascicular area in rat. Neuroscience 2006b;138:197–220. [PubMed: 16361065]

Ward HL, Small CJ, Murphy KG, Kennedy AR, Ghatei MA, Bloom SR. The actions of tuberoinfundibular peptide on the hypothalamo-pituitary axes. Endocrinology 2001;142:3451–3456. [PubMed: 11459790]

Webster WR. Central neural mechanisms of hearing. Proc Aust Physiol Pharmacol Soc 1977;8:1–7.

Winer JA, Larue DT, Diehl JJ, Hefti BJ. Auditory cortical projections to the cat inferior colliculus. J Comp Neurol 1998;400:147–174. [PubMed: 9766397]

Wünscher, W.; Shober, W.; Werner, L. Architectonisher atlas vom hirnstamm der ratte. S. Hirzel; Leipzig: 1965.

Yeomans JS, Li L, Scott BW, Frankland PW. Tactile, acoustic and vestibular systems sum to elicit the startle reflex. Neurosci Biobehav Rev 2002;26:1–11. [PubMed: 11835980]

Zhao ZQ, Duggan AW. Idazoxan blocks the action of noradrenaline but not spinal inhibition from electrical stimulation of the locus coeruleus and nucleus Kölliker-Fuse of the cat. Neuroscience 1988;25:997–1005. [PubMed: 3405439]

Zhou J, Shore S. Convergence of spinal trigeminal and cochlear nucleus projections in the inferior colliculus of the guinea pig. J Comp Neurol 2006;495:100–112. [PubMed: 16432905]

Zilles, K.; Wree, A. Cortex: areal and laminar structure.. In: Paxinos, G., editor. The rat nervous system. Academic Press; Sydney: 1985. p. 375-415.

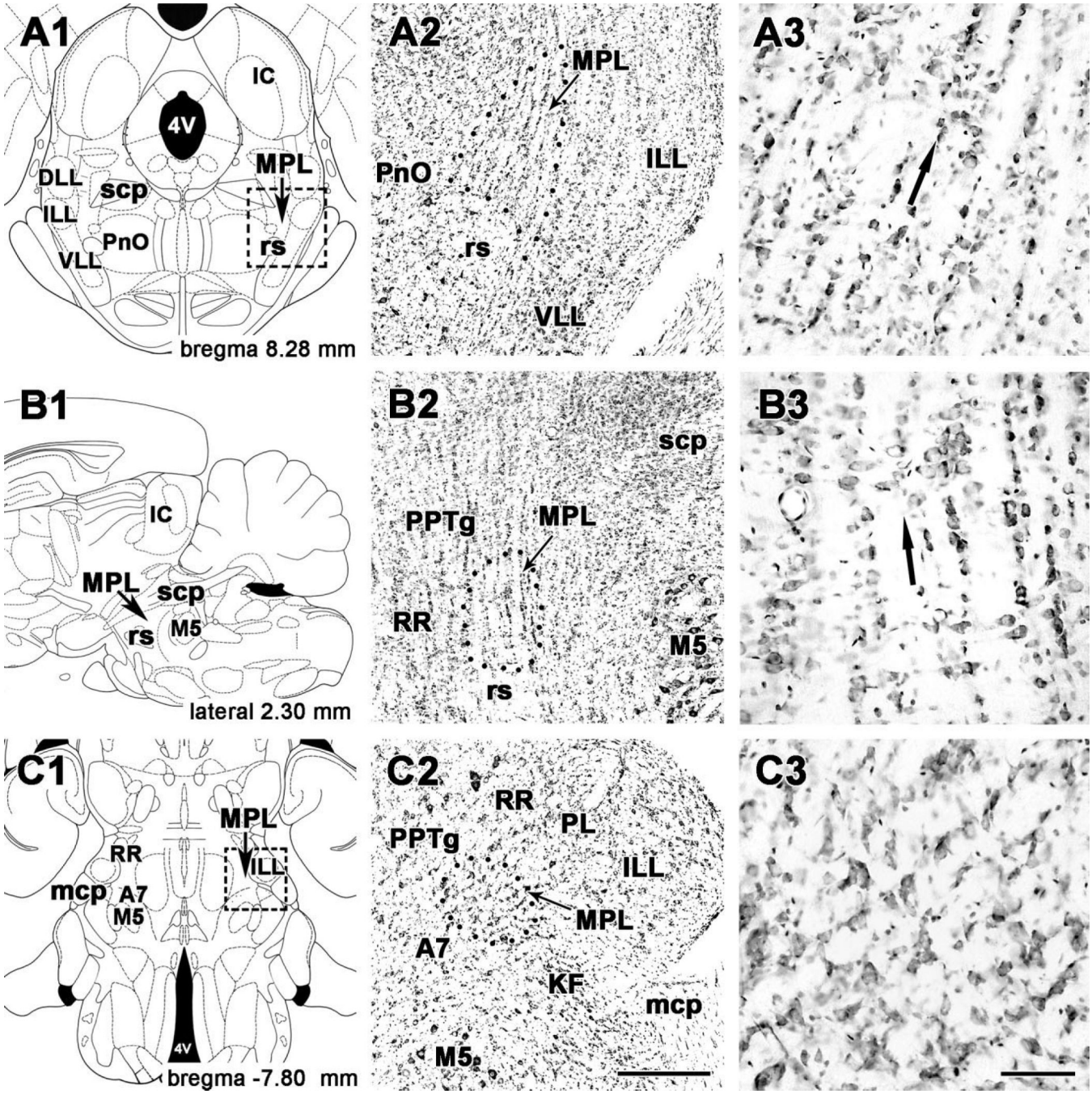


**Fig. 1.**

The cytoarchitecture of the medial paralemniscal nucleus in cresyl-violet stained sections. **A1–A3:** Coronal sections. **B1–B3:** Sagittal sections. **C1–C3:** Horizontal sections. Drawings on the left (A1, B1, C1) are modifications of panels in rat brain stereotaxic atlases (Paxinos and Watson, 1998, 2005). Panels in the middle (A2, B2, C2) correspond to the area containing MPL in the drawings. Dotted lines indicate the cytoarchitectonic borders of MPL. Panels on the right (A3, B3, C3) are high-magnification photomicrographs of MPL shown in the middle panels. Small arrows point to the medial paralemniscal nucleus, and large arrows in the right panels indicate the orientation of cell columns in the MPL. For abbreviations, see list. Scale bar = 500 μm in C2 (applies to A2–C2); 100 μm in C3 (applies to A3–C3).

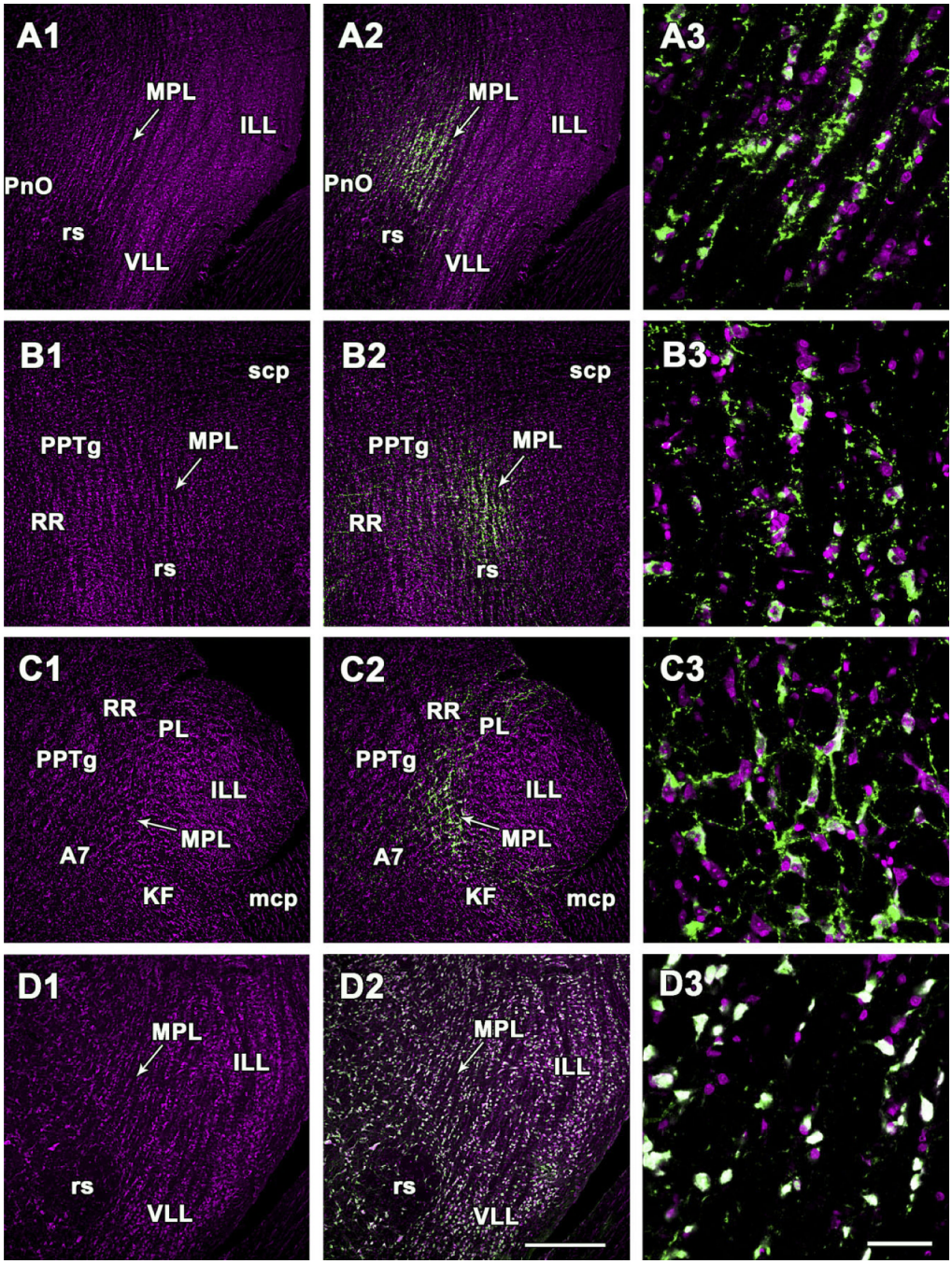


**Fig. 2.**

Demonstration of TIP39- and NeuN-immunoreactive neurons in the cytoarchitectonically defined medial paralemniscal nucleus. A1–A3, D1–D3: Coronal sections. B1–B3: Sagittal sections. C1–C3: Horizontal sections. **A1,B1,C1,D1:** Sections are stained with the red fluorescent Nissl dye, and the picture is artificially made magenta. Arrows point to the medial paralemniscal nucleus. **A2,B2,C2:** The position of TIP39 neurons is demonstrated by green fluorescent immunolabeling in the same field of the same sections as A1, B1, and C1. **D2:** The same field as D1 is shown double labeled with the red fluorescent Nissl dye (magenta) and NeuN (green). The Nissl dye and NeuN co-localizes in all the neurons indicated by their white color. A3, B3, C3, and D3 are high-magnification confocal photomicrographs. The fields

correspond to MPL in the middle panels. For abbreviations, see list. Scale bar = 500 μm in D2 (applies to A1–D2); 100 μm in D3 (applies to A3–D3).

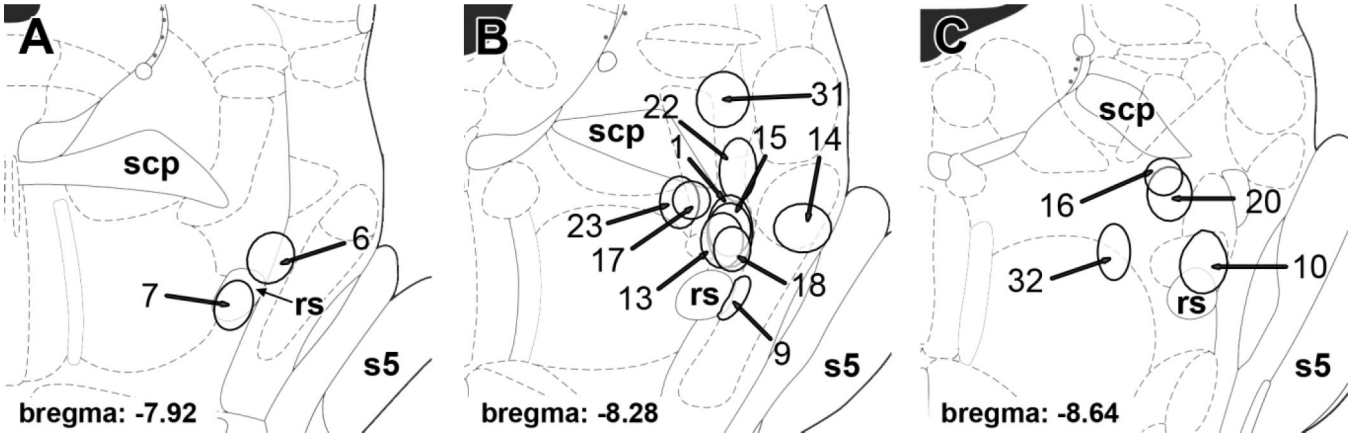


**Fig. 3.**

Locations and sizes of cholera toxin B subunit (CTB) injections into and around the MPL. **A,C:** Brain sections at –7.92 mm (A), and –8.64 mm (C) from the level of the bregma show control injection sites rostral (A) and caudal (C) to the MPL, respectively. **B:** Brain section at –8.28 mm shows injection sites in the MPL and control injection sites into adjacent areas. The numbers of injection sites correspond to the animal's number in the protocol of the study. The drawings of brains are adapted and modified from the atlas of Paxinos and Watson (2005). For abbreviations, see list.

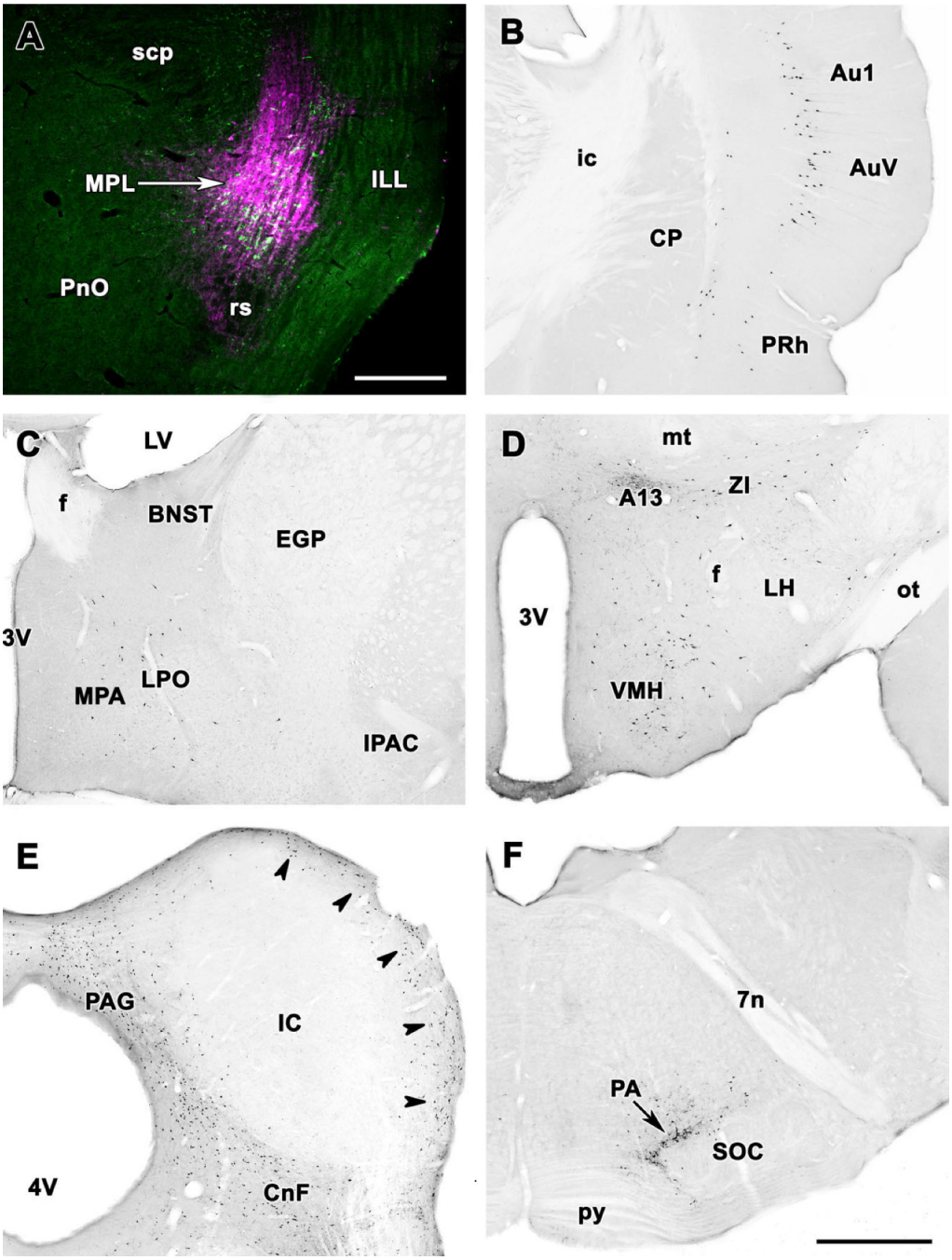


**Fig. 4.**

Topographical distrbution of retrogradely labeled neurons after CTB injection into the MPL. **A:** The CTB injection site (magenta) is shown in relation to TIP39-immunoreactive neurons (green) in a double fluorescent labeled coronal section. The injection site covers most of the MPL. B–F: Photomicrographs of coronal sections single labeled with DAB immunocytochemistry demonstrate retrogradely labeled neurons in the same brain. **B:** A high density of retrogradely labeled neurons is shown in layer V of the primary auditory cortex and the ventral secondary auditory cortex. Labeled cells in a lower density are present in layers Vi and V of the perirhinal cortex and layer VI of the ventral secondary auditory cortex. **C:** Retrogradely labeled neurons are distributed in the preoptic region. **D:** A high density of

retrogradely labeled neurons in the ventrolateral subdivision of the hypothalamic ventromedial nucleus, the dorsolateral hypothalamic area, the area of the A13 dopamine cell group, and the zona incerta. Scattered cells are also present in the lateral hypothalamus. **E:** Retrogradely labeled neurons are abundant in the dorsal periaqueductal gray, the cuneiform nucleus, and the external cortex of the inferior colliculus (arrowheads). In contrast, the central nucleus of the inferior colliculus is devoid of labeled neurons. **F:** Retrogradely labeled cells are concentrated in the periolivary area immediately dorsal to the superior olive. For abbreviations, see list. Scale bar = 500 μm in A; 1 mm in F (applies to B–F).

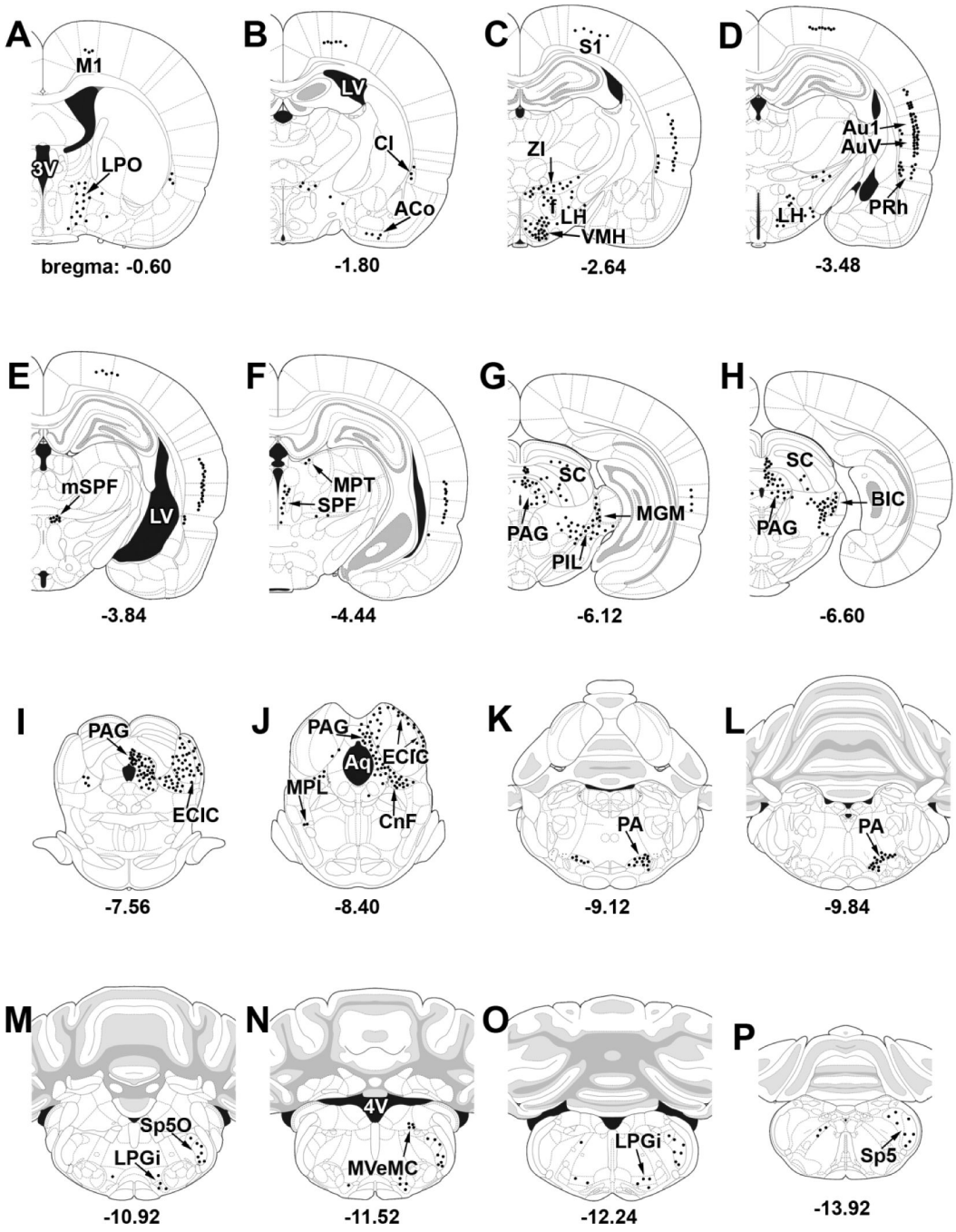


**Fig. 5.**

**A–P:** Schematic illustrations of the afferent connections of the MPL. The distribution of CTB-containing cells following CTB injections restricted to the MPL is from injections No. 1, 13, 15, and 18, shown in Figure 3. Dots represent labeled cells in corresponding single 50-μm sections. For abbreviations, see list.

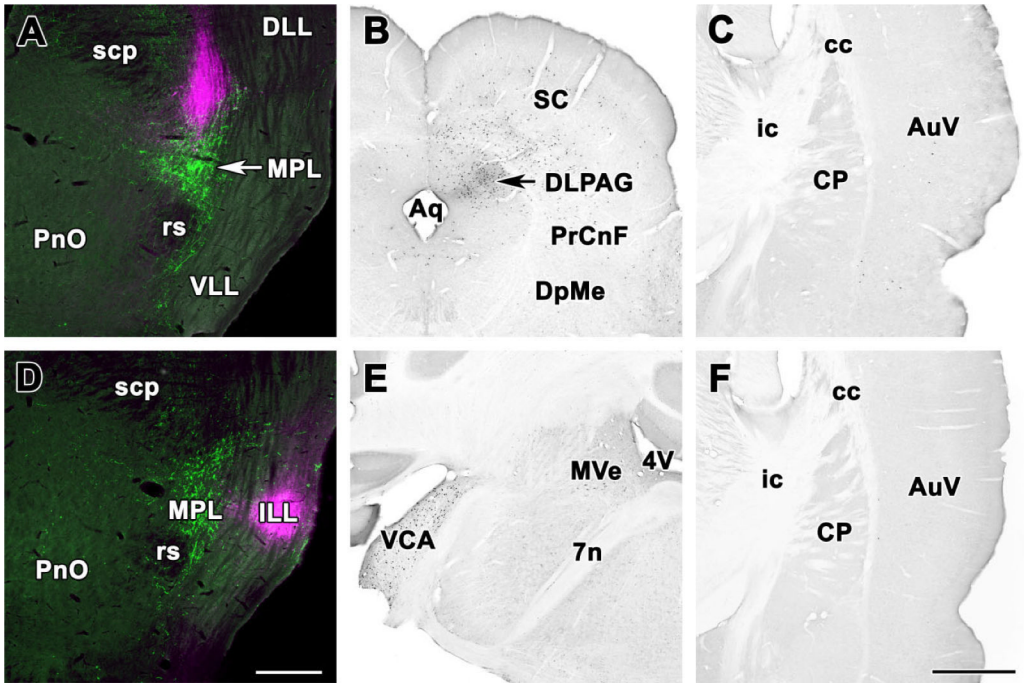


**Fig. 6.**

Location of retrogradely labeled neurons following control injections into areas adjacent to the MPL. **A:** Injection into the paralemniscal region immediately dorsal to the MPL. The CTB injection site (magenta) overlaps only slightly with the MPL containing TIP39-immunoreactive neurons (green). **B:** Photomicrographs of coronal sections single labeled with DAB immunocytochemistry demonstrate retrogradely labeled neurons in the periaqueductal gray and the superior colliculus of the same brain. **C:** In contrast, the auditory cortex contains only a few labeled neurons. **D:** Injection into the intermediate nucleus of the lemniscus lateralis. The CTB injections site (magenta) is located lateral to the MPL containing TIP39-immunoreactive neurons (green). **E:** Photomicrographs of coronal sections single labeled with DAB immunocytochemistry demonstrate a very high number of retrogradely labeled neurons in the contralateral ventral cochlear nucleus and a less moderate labeling in the magnocellular medial vestibular nucleus of the same brain. **F:** In contrast, the auditory cortex contains no labeled neurons. For abbreviations, see list. Scale bar = 500 μm in D (applies to A,D); 1 mm in F (applies to B,C,E,F).

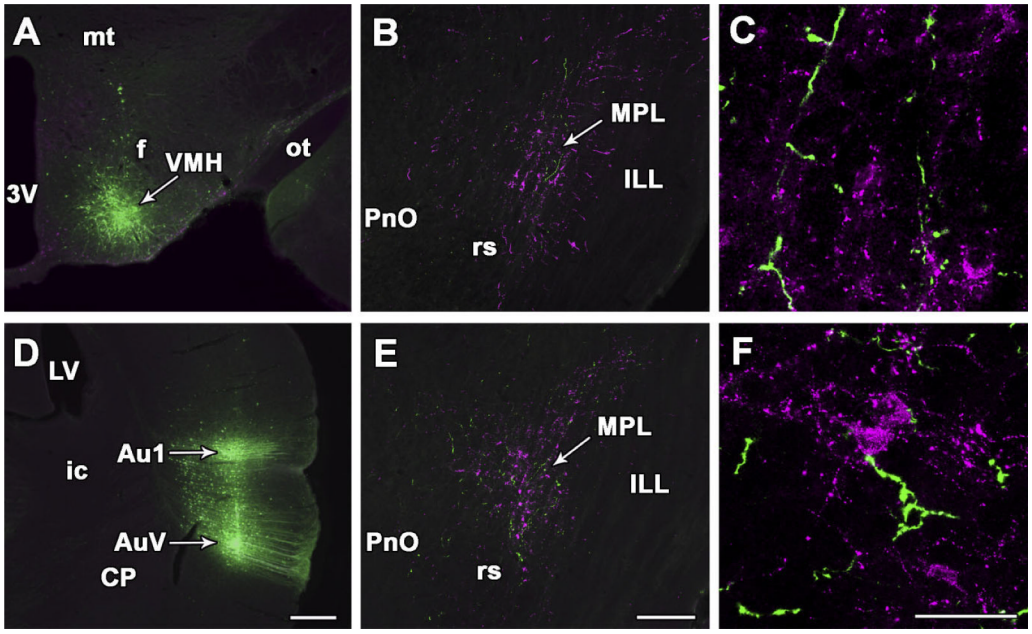


**Fig. 7.**

Projections from the hypothalamic ventromedial nucleus and the auditory cortex to the MPL. **A:** BDA injection site in the ventrolateral subdivision of the hypothalamic ventromedial nucleus. **B:** In the same brain, anterogradely labeled fibers (green) are distributed among TIP39-immunoreactive neurons (magenta) in the MPL. **C:** High-magnification confocal images suggest BDA-containing nerve terminals in the MPL. **D:** BDA injection sites in the primary and secondary auditory cortices. **E:** In the same brain, anterogradely labeled fibers (green) are distributed among TIP39-immunoreactive neurons (magenta) in the MPL. **F:** High-magnification confocal images suggest BDA-containing nerve terminals in the MPL. For abbreviations, see list. Scale bar = 500 μm in D (applies to A,D); 300 μm in E (applies to B,E); 50 μ in F (applies to C,F).

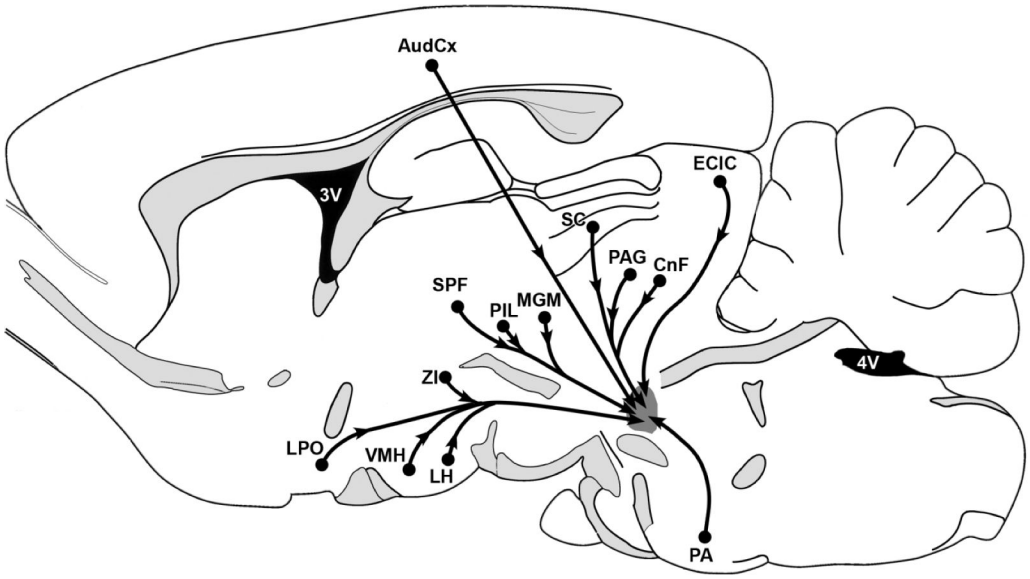


**Fig. 8.**

Schematic **s**ummary of brain areas that send significant projection to the MPL. A projection was considered significant if more than five retrogradely labeled cells were present in a section of the area following the injection of retrograde tracer into the MPL. Projections are indicated from the auditory cortex, the lateral preoptic area, the hypothalamic ventromedial nucleus, the lateral hypothalamic area, the subparafascicular area of the thalamus, the posterior intralaminar thalamic nucleus, the medial nucleus of the medial geniculate body, the zona incerta, deep layers of the superior colliculus, the periaqueductal gray, the cuneiform nucleus, the external cortex of the inferior colliculus, and the periolivary area. For abbreviations, see list.

**TABLE 1**

Brain Areas Containing Retrogradely Labeled Cells Following Cholera Toxin B (CTB) Injection Into the Medial Paralemniscal Nucleus[1]

| Area | Density |
|---|---|
| Forebrain | |
| Cerebral cortex | |
| Prefrontal cortex | 0 |
| Somatomotor cortex | + |
| Somatosensory cortex | + |
| Visual cortex | 0 |
| Auditory cortex | |
| Primary auditory cortex | ++ |
| Secondary auditory cortex ventral part | +++ |
| Secondary auditory cortex dorsal part | ++ |
| Ectorhinal cortex | + |
| Perirhinal cortex | ++ |
| Insular cortex | + |
| Claustrum | + |
| Hippocampus | 0 |
| Amygdala | |
| Anterior cortical nucleus | + |
| Septum | 0 |
| Caudate-putamen | 0 |
| Basal forebrain | 0 |
| Diencephalon | |
| Thalamus | |
| Subparafascicular area | ++ |
| Posterior intralaminar thalamic nucleus | ++ |
| Peripeduncular nucleus | ++ |
| Supragenicular nucleus | ++ |
| Medial geniculate body | |
| Medial nucleus | ++ |
| Subthalamic nucleus | 0 |
| Hypothalamus | |
| Lateral preoptic area | ++ |
| Medial preoptic area | + |
| Dorsal hypothalamic area | + |
| Lateral hypothalamic area | |
| Juxtaparaventricular part | ++ |
| Tuberal part | ++ |
| Peduncular part | ++ |
| Perifornical area | ++ |
| Hypothalamic ventromedial nucleus | |
| Ventrolateral subdivision | +++ |

| Area | Density |
|---|---|
| Central subdivision | ++ |
| Dorsomedial subdivision | + |
| Zona incerta | ++ |
| Midbrain | |
| Medial pretectal nucleus | + |
| Olivary pretectal nucleus | + |
| Periaqueductal gray | |
| Dorsomedial subdivision | +++ |
| Dorsolateral subdivision | ++ |
| Lateral subdivision | +++ |
| Ventrolateral subdivision | ++ |
| Deep mesencephalic nucleus | ++ |
| Superior colliculus | |
| Superficial layers | 0 |
| Intermediate layers | + |
| Deep layers | ++ |
| Inferior colliculus | |
| Central nucleus | 0 |
| Dorsal cortex | ++ |
| External cortex | +++ |
| Nucleus of the brachium | ++ |
| Precuneiform area | ++ |
| Cuneiform nucleus | +++ |
| Pons | |
| Medial paralemniscal nucleus, contralateral | ++ |
| Nucleus of the central acoustic tract | + |
| Periolivary area | ++ |
| Superior paraolivary nucleus | + |
| Parabrachial nuclei | + |
| Medial vestibular nucleus | |
| Magnocellular part | + |
| Medulla oblongata | |
| Lateral paragigantocellular nucleus | + |
| Spinal trigeminal nucleus | + |
| Intermediate reticular nucleus, contralateral | + |
| Cerebellum | 0 |

[1] Brain regions where we did not observe labeled cells are not included or are marked with 0 density. +, 1-5 cells/section; ++, 6-15 cells/section; +++, more than 15 cells/section.